Linking Parenchymal Disease Progression to Changes in Lung Mechanical Function by Percolation

Jason H. T. Bates[1,2], Gerald S. Davis[1,2], Arnab Majumdar[3], Kelly J. Butnor[1,2], and Béla Suki[3]

[1]Vermont Lung Center, University of Vermont College of Medicine and [2]Fletcher Allen Health Care, Burlington, Vermont; and [3]Department of Biomedical Engineering, Boston University, Boston, Massachusetts

Rationale: **The mechanical dysfunction accompanying parenchymal diseases such as pulmonary fibrosis and emphysema may follow a different course from the progression of the underlying microscopic pathophysiology itself, particularly in the early stages. It is tempting to speculate that this may reflect the geographical nature of lung pathology. However, merely ascribing mechanical dysfunction of the parenchyma to the vagaries of lesional organization is unhelpful without some understanding of how the two are linked.**

Objectives: **We attempt to forge such a link through a concept known as percolation, which has been invoked to account for numerous natural processes involving transmission of events across complex networks.**

Methods: **We numerically determined the bulk stiffness (corresponding to the inverse of lung compliance) of a network of springs representing the lung parenchyma. We simulated the development of fibrosis by randomly stiffening individual springs in the network, and the development of emphysema by preferentially cutting springs under the greatest tension.**

Measurements and Main Results: **When the number of stiff springs was increased to the point that they suddenly became connected across the network, the model developed a sharp increase in its bulk modulus. Conversely, when the cut springs became sufficiently numerous, the elasticity of the network fell to zero. These two conditions represent percolation thresholds that we show are mirrored structurally in both tissue pathology and macroscopic computed tomography images of human idiopathic fibrosis and emphysema.**

Conclusions: **The concept of percolation may explain why the development of symptoms related to lung function and the development of parenchymal pathology often do not progress together.**

Keywords: pulmonary fibrosis; emphysema; lung function; abnormal histology; high-resolution computed tomography

AT A GLANCE COMMENTARY

Scientific Knowledge on the Subject

There is a great deal known about the pathophysiology of pulmonary fibrosis and emphysema, and percolation is well studied in the physics literature. However, the link between these fields is relatively unstudied.

What This Study Adds to the Field

The concept of percolation can help to link progression of parenchymal pathophysiology to development of clinical symptoms.

There is great variability in the extent to which progression of parenchymal disease is linked to alterations in lung function. In some cases, worsening lung mechanics seem to go hand in hand with disease progression. For example, serial measurements of forced vital capacity have been shown to be predictive of survival in patients with idiopathic pulmonary fibrosis (IPF) (1), whereas an accelerated decline in lung function is a well-known feature of adverse prognosis in chronic obstructive pulmonary disease (2). On the other hand, it has been shown that physiological variables may change minimally during progression of IPF before a sudden clinical decline preceding death (3). Similarly, smokers may develop emphysematous changes evident on high-resolution computed tomography (CT) before exhibiting clinical symptoms or abnormal lung function (4, 5). These observations suggest that the mechanical dysfunction accompanying parenchymal disease may follow a different course from the progression of the underlying pathologic morphology, particularly in the early stages.

In considering how lung mechanical function might progress relative to parenchymal disease itself, we note that characteristic spatial organization is a recognized feature of many lung pathologies (6–8). For example, cardiac or hydrostatic pulmonary edema frequently involves relatively uniform fluid accumulation in interstitial and alveolar spaces, apart from a gravity-dependent accentuation in dependent lung zones (9). By contrast, IPF is manifested pathologically as usual interstitial pneumonitis with a predilection for basal subpleural locations, and begins with isolated lesions that increase in size and number over time until they eventually coalesce (10). Similarly, the initial lesions of emphysema, either centrilobular or panlobular, are also diffusely scattered throughout the lung (11). Spatial organization is also not just a feature of parenchymal pathology. Even the link between structure and function in normal lung tissue depends critically on the way in which the tissue constituents are arranged with respect to each other. For example, the progressive stiffening of the lung with increasing volume reflects the increasing stress-bearing role of collagen fibers as they become straightened and take over from their colocalized elastin fibers. The mechanical properties of the lung thus do not resemble the properties of either fiber type alone (12, 13).

It is therefore apparent that the geographical nature of lung pathology should exert an important influence on its physiological manifestations. Nevertheless, merely ascribing mechanical dysfunction of the parenchyma to the vagaries of lesional organization is unhelpful without an understanding of how the two are linked. In the present article, we attempt to forge such a link through a concept known as percolation, which has been invoked to account for numerous natural processes involving transmission of events across networks (14–16). Using an elastic

(*Received in original form November 30, 2006; accepted in final form June 14, 2007*)

Supported by National Institutes of Health grants R01 HL67273, HL75593, HL59215, and NCRR P20 RR15557.

Correspondence and requests for reprints should be addressed to Jason H.T. Bates, Ph.D., HSRF 228, 149 Beaumont Avenue, Burlington, VT 05405-0075. E-mail: jason.h.bates@uvm.edu

This article has an online supplement, which is accessible from this issue's table of contents at www.atsjournals.org

Am J Respir Crit Care Med Vol 176. pp 617–623, 2007
Originally Published in Press as DOI: 10.1164/rccm.200611-1739OC on June 15, 2007
Internet address: www.atsjournals.org

network model of the parenchyma, we show that as isolated lesions increase in number they suddenly reach a point, known as the percolation threshold, at which they become connected in a continuous pathway across an expanse of lung tissue. At this threshold, the tissue undergoes a sharp change in its bulk mechanical properties. We conclude that percolation can explain why there is often a disconnect between the progression of parenchymal pathology and the development of clinical symptoms related to lung function. Some of the results of this studies have been previously reported in the form of an abstract (17).

METHODS

We modeled the lung parenchyma as a two-dimensional network of ideal linearly elastic springs with spring constants of 1 (arbitrary units) and a rectangular boundary arranged in a hexagonal array. The outer borders of the network were held fixed to represent a fixed lung volume. Initially, the elastic constants and unstressed lengths of the springs were identical, so the baseline network configuration was uniform. The individual spring constants were then varied, and the equilibrium configuration of the network was calculated by minimizing the elastic energy (E) of the spring array, using a process similar to simulated annealing (18), which is a numerical technique mimicking the gradual cooling of atoms in a metal or glass. Starting from some initial configuration, the total energy of the network was calculated as the sum of all individual spring energies, each given by half the product of the spring constant times the square of the extension beyond equilibrium length. Each spring junction point was then moved a small distance in the direction of the net force acting on it and E was recalculated. If the change in energy (ΔE) was negative, the new configuration was accepted. However, to reduce the likelihood of the energy solution becoming trapped in a local minimum we also occasionally accepted configurations for which $\Delta E > 0$, the probability of acceptance being $P = \exp(-\Delta E/T)$, where T is a control parameter analogous to temperature. These steps were repeated until a convergence criterion was reached (i.e., $\Delta E/E$ remained lower than 10^{-7} for 20 consecutive iterations). The value of T was then reduced by 1%, followed by further iterations. This process was repeated 1,000 times, resulting in a total number of iterations between 25,000 and 40,000. Further details can be found in Cavalcante and coworkers (18).

We calculated the two-dimensional bulk modulus (B) of the network by increasing its linear dimensions biaxially by 0.001%, and then recalculating the new equilibrium configurations of all the springs. The resulting increase in stress (ΔS = increase in force per unit length and unit thickness) was then divided by the increase in linear strain ($\Delta e = 0.00001$) to yield $B = \Delta S/\Delta e$. B is thus a measure of the overall stiffness of the network, and is thus the model equivalent of the inverse of lung compliance. The borders of the network were set so that at its minimal energy configuration each spring was stretched to a value of 2.3 of its unstressed length. This degree of initial stretch was chosen arbitrarily to allow for reasonably large changes in network configuration to occur after either stiffening or cutting of springs, yet still allow for rapid convergence of the preceding energy minimization algorithm.

To simulate the collagen deposition that occurs in fibrotic lung disease, the elastic constants in a network of 1,171 springs were increased randomly by a factor of 100. To simulate emphysema we used a much larger network of 67,276 springs in which, rather than cutting the springs randomly, we invoked the notion that alveolar walls experiencing high stress are more likely to break than walls under less stress (19). We therefore began the simulation by randomly breaking 1% of the springs (673 springs) in the network to seed the destructive process. We then determined the new equilibrium configuration of the network and chose to cut the next 81 springs that were under the greatest stress. This was repeated until B fell to zero.

RESULTS

The value of B (equivalent to the inverse of lung compliance) for our spring network model of fibrosis as a fraction of randomly stiffened springs is shown in Figure 1. B changes relatively slowly when the fraction of stiff springs is below about 0.6 and much more quickly when the replaced fraction is above 0.6. The knee in the relationship, at about the 60% replacement point, indicates a percolation threshold separating widely differing rates of change of mechanical function. For comparison, we also include in Figure 1 a diagonal straight line corresponding to the constant rate of change in B occurring when the stiffness of each spring in the network increases progressively and simultaneously. Also shown in Figure 1 are example configurations of our network model at baseline (uniform spring stiffnesses) and when the model has two different fractions of stiff springs (*see* the online supplement for additional network images). When about 50% of the springs are stiffened they clump together in groups that are still separated by springs having the original lower stiffness. By the time 65% of the springs are stiffened, they span the network both vertically and horizontally in unbroken chains. Note how the network begins in a homogeneous configuration at 0%, and becomes increasingly heterogeneous as the springs are stiffened. Heterogeneity of the network reaches a maximum when about 60% of the springs have been stiffened, and then decreases beyond this point until all the springs have been stiffened, at which point the network returns to perfect homogeneity.

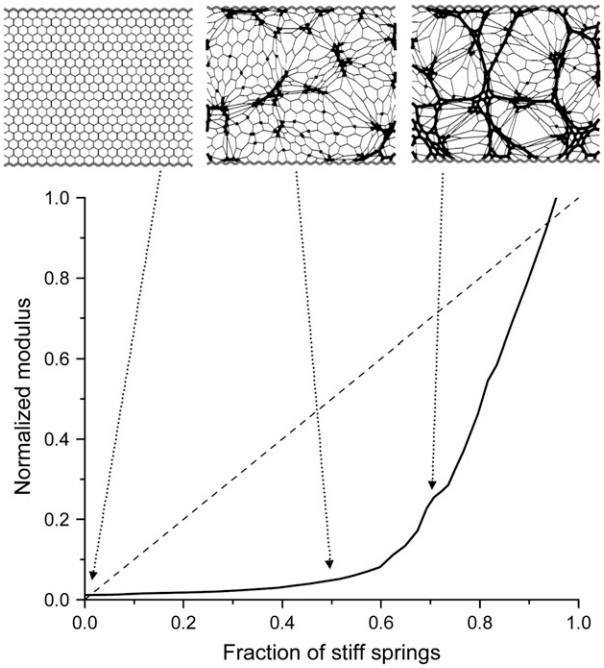

Figure 1. Simulation of the progression of pulmonary fibrosis. The curve shows the bulk modulus of the elastic network versus the fraction of springs randomly stiffened by a factor of 100 (normalized to the modulus of the network when all springs are stiffened). If all the spring constants were uniformly stiffened in a gradual manner from the baseline value of 1 to 100, the modulus would follow the *dashed diagonal line*. *Top*: Network configurations obtained when 0, 50, and 67% of the springs have been stiffened (*see* the online supplement).

The simulation of the progression of emphysema is shown in Figure 2 (*see* the online supplement for additional network images). Here, the cutting of the springs was not random, as was the stiffening in the fibrosis simulation in Figure 1, but rather was targeted to those springs with the highest stress (once the process had been seeded by a small amount of purely random cutting). This caused the holes in the network to be spatially correlated and made B fall toward zero much more rapidly than if all the cutting had been completely random. Figure 2 shows the progression of B with fraction of cut springs and demonstrates an

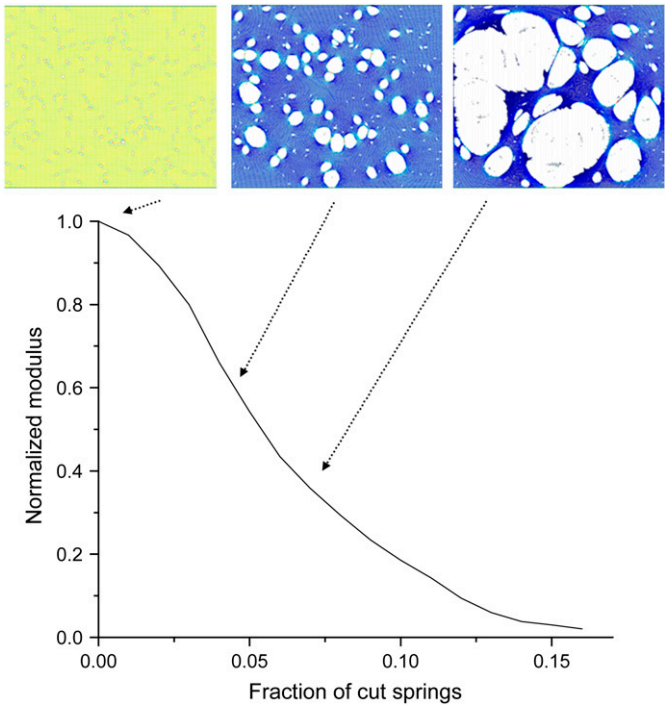

Figure 2. (*A*) Simulation of the progression of emphysema. The *curve* shows the bulk modulus of the elastic network (normalized to the modulus of the network when fully intact) versus the fraction of springs cut on the basis of the amount of tension they carry (*see* text for details). *Top*: Network configurations obtained at three points along this process. The stresses in the individual springs are indicated by color coding, with *yellow* indicating high stress and decreasing stress corresponding to progressively darker shades of *blue* (*see* the online supplement).

initially accelerating rate of decline that eventually decelerates as stiffness approaches zero, when about 15% of the springs have been cut. The point at which B = 0 represents another percolation threshold, this time corresponding to the complete loss of network elasticity. Also shown are three examples of the network itself, which show how an initial set of randomly located small holes progresses to a series of large holes that span the network in an almost contiguous pathway. The heterogeneity of the structure increases as the network undergoes progressive breakdown.

DISCUSSION

Percolation describes the process whereby something picks its way randomly through a labyrinth of obstacles under the influence of some driving force. Whether or not the labyrinth is completely traversed depends on a variety of factors such as the density and spatial organization of obstacles and the nature of the force. These factors together determine the so-called percolation threshold, which is the set of conditions under which traversal of the labyrinth is only just achieved. Percolation is a well-studied phenomenon that has been invoked to account for the progression, or lack of it, of many complex processes in nature such as forest fires (20), infectious disease epidemics (14), and blood capillary formation (15). The importance of the percolation threshold in these examples is that it can help in understanding when a fire will burn out an entire forest, when a disease will develop into an epidemic, or when a tissue will become adequately perfused. The percolation threshold is thus an example of an emergent property, something that arises within a complex system not just as a result of the specific components involved, but in large part because of the way these components are arranged within the system.

The elasticity of lung tissue is also an emergent property in the sense that it arises in a nonobvious way from the ensemble behavior of a network of protein fibers (12, 21) acting in concert with the surface tension of an air–liquid interface (21). Importantly, the elasticity of the lung as a whole does not resemble that of any of its individual components on their own. For example, we have previously invoked a percolation-like process to explain the strain stiffening of lung tissue strips, which we modeled as a network of collagen–elastin fiber pairs that exhibits a sudden increase in elastic modulus near the point at which stress-bearing collagen fibers appear in a continuous pathway from one end of the network to the other (22). Other studies have shown that when springs are randomly connected between neighboring vertices in a two-dimensional lattice, the lattice will suddenly assume a finite stiffness when a set of springs appears that percolates contiguously across the lattice (16, 23). We were therefore led to ask whether pathological changes in lung stiffness might also be understood as an emergent phenomenon arising through percolation, particularly in view of the fact that many parenchymal diseases begin with the appearance of a few isolated lesions that progress to eventually engulf much, if not all, of the organ. At some point during this process we would expect the lesions to reach a critical density at which they form an unbroken pathway that percolates from one boundary of the lung to another. The boundaries involved could be any that define a structurally coherent region of the lung, from intralobular septa all the way up in scale to diametrically opposite pleural surfaces. Obviously, reaching the percolation threshold across the entire lung could result in a dramatic downturn in lung function. However, we might also expect a sudden effect on function if percolation occurred across any important subsegment of the lung, particularly if it affects the integrity of the parenchymal link between the axial and peripheral fiber networks of the lung that are thought to bear much of the stress during lung inflation (24).

The percolation concept supported by our simulations of the progression of fibrosis shows (Figure 1) that the bulk stiffness of a network does not increase linearly as progressively more individual springs in the network are altered. Instead, B increases rather slowly at first until the percolation threshold is reached, at which point contiguous pathways of altered stiffness begin to span the entire network. At this point, B starts to increase at a greatly accelerated rate. These simulations suggest that the early lesions of fibrosis may manifest with minimal functional consequences until they progress to the point of spanning significant portions of the lung in a connected fashion (i.e., at the percolation threshold). At this point, we predict there will be a marked increase in symptoms associated with lung function and the work of breathing, presaging a rapid decline in patient status. This could explain, for example, why patients with IPF have been observed to have stable physiological parameters for periods of many months before experiencing precipitous declines just before death (3).

The functional consequences of percolation in emphysema are also evident in our network model, which predicts that the very early stages of emphysema may be associated with a modest rate of decline in lung function (the shoulder on the modulus curve by the *left-hand arrow* in Figure 2), as has been described in patients (4, 5, 25) and mice (26). Soon, however, the rate of decline in lung recoil predicted by our model becomes more pronounced (between the *left-hand* and *middle arrows* in Figure 2), which is what has been observed in both smokers and ex-smokers (27, 28) and to a much lesser extent even in normal individuals (2, 28). Beyond the maximal rate of decline, over the

lower portion of the curve, parenchymal destruction becomes overwhelming and the modulus approaches zero. This stage of destruction would already be incompatible with life, were it to describe the entire lung. On the other hand, the lower part of the curve may account for the behavior of subregions of the lung. That is, so long as local B for some region of the lung is greater than zero, the region is able to maintain at least some recoil pressure. Once B approaches zero, however, we reach what is effectively another percolation threshold, characterized by the sudden inability of the tissue to maintain any degree of integrity, at which point it retracts into a single bulla (*see, e.g.*, Figure 2 of Shapiro and Ingenito [29]). Interestingly, the predicted decrease in network stiffness (Figure 2) occurs very rapidly overall, in the sense that it takes only a little more than 15% of the springs to be cut before the modulus reaches zero. However, the fraction of the lung area occupied by holes becomes much greater than the 15% of springs that have been cut. These effects are due to the fact that the springs are cut according to the tension they carry, so that holes tend to become amplified as the stress is transmitted from walls to neighboring walls after rupture (19). This process may explain the progressive nature of emphysema (19, 29).

The relevance of our network model to the progression of diseases such as pulmonary fibrosis and emphysema is more than merely functional, however. The altered structures of the networks shown in Figures 1 and 2 also bear striking resemblances to the histological pictures of both diseases. This is exemplified in Figure 3, which shows representative pathology specimens of lung biopsy tissues obtained from the surgical pathology files of Fletcher Allen Health Care (Burlington, VT). Sections were cut from resected tissue specimens that had been inflated with formalin and then embedded in paraffin. The sections were stained with hematoxylin and eosin, and photographed by light microscopy. Normal lung tissue consists of relatively uniform alveoli punctuated by alveolar ducts, small airways, and blood vessels, and alveolar septal thickness is relatively uniform (Figure 3, *top left*). The example of edema (Figure 3, *top right*) shows uniform septal thickening and flooding of the alveolar spaces with proteinaceous fluid but no apparent change in the connectivity of the alveolar septal network. If these changes were uniform throughout the lung, edema might be appropriately modeled by uniform stiffening of all springs in the network. On the other hand, edema is likely a heterogeneous process in which some alveoli fill with fluid before others, which should be modeled by stiffening only a fraction of the network springs. By contrast, there is no doubt about the importance of spatial heterogeneity in the emphysema (Figure 3, *right middle* and *bottom*) and fibrosis (Figure 3, *left middle* and *bottom*) specimens, which show wide geographic variations in both septal thickness and airspace size. Next to the fibrosis and emphysema specimens we show the same images in black and white to more clearly relate their structures to the mechanism of percolation. On the black-and-white images of mild disease, we indicate isolated islands of septal thickening (fibrosis) and airspace enlargement (emphysema). On the black-and-white images of severe disease, we indicate regions where these features have completely traversed across the images. For fibrosis, it is the stiff collagen-dense regions (pathways marked with *yellow lines*) that percolate, whereas for emphysema, it is the airspaces without alveolar septal walls (pathways marked with *green lines*) that percolate. These images thus show how mild and severe parenchymal disease can be placed below and above, respectively, a structural percolation threshold.

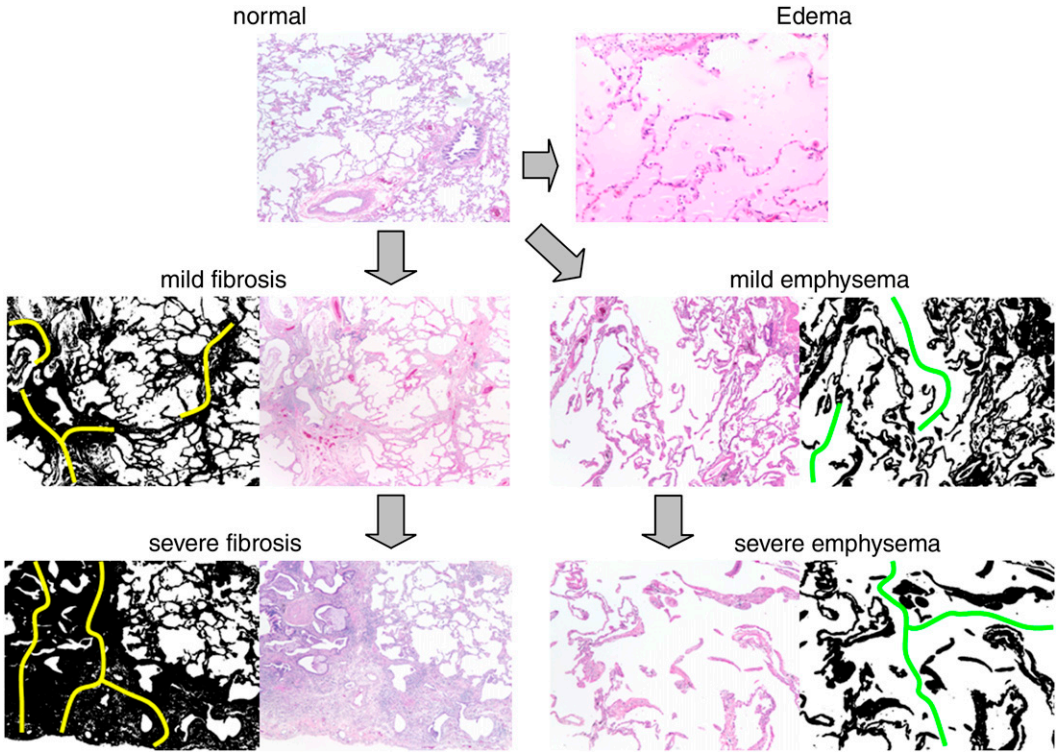

Figure 3. Lung pathology illustrates the concepts of diffuse or focal disease and percolation at a microscopic level. Representative lung biopsy sections were inflated by injection with formalin, sectioned, stained with hematoxylin and eosin, and photographed. Normal lung tissue (*top left*; original magnification, ×40) shows numerous delicate alveolar walls and relatively uniform airspace diameters. Cardiogenic pulmonary edema (*top right*; original magnification, ×200) demonstrates generalized alveolar filling with proteinaceous material. Mild usual interstitial pneumonitis (UIP) (*middle left*; original magnification, ×40) shows focal areas of cellular accumulations and fibrosis with adjacent areas of relatively normal lung, whereas severe UIP (*bottom left*; original magnification, ×40) shows extensive dense fibrosis that spans the microscopic field. Mild emphysema (*middle right*; original magnification, ×100) demonstrates enlarged airspaces scattered throughout the normal tissue with fragmentation of occasional alveolar walls, whereas severe emphysema (*bottom right*; original magnification, ×200) shows extensive widely linked enlarged airspaces and most alveolar walls are fragmented. Next to the fibrosis and emphysema specimens, the same images are shown in high-contrast black and white. *Yellow lines* indicate isolated islands of septal thickening in mild fibrosis and thickening that has completely traversed the tissue in severe fibrosis. For the emphysema images, *green lines* indicate airspace enlargement that is patchy in mild disease and contiguous in severe disease.

Support for percolation as a relevant organizational principle in parenchymal lung disease is also apparent at the level of the whole lung. Figure 4 shows high-resolution CT images of representative cases obtained from the radiology files of Fletcher Allen Health Care. The normal lung (Figure 4, *top left*) exhibits a uniform gray parenchyma with small structures of higher attenuation representing bronchovascular bundles, septal planes, and larger blood vessels or airways. In pulmonary edema (Figure 4, *top right*), one sees branches of high attenuation, presumably corresponding to engorged vessels, superimposed on an almost uniformly increased parenchymal opacity. By contrast, even in mild IPF (Figure 4, *middle left*), the normal parenchymal uniformity is interrupted by larger and more numerous reticular opacities, particularly adjacent to some of the pleural surfaces. In severe fibrosis (Figure 4, *bottom left*), these opacities form a dense patchwork that connects across the entire lung field, even though one can still see regions of apparently normal parenchyma. These features closely resemble the structure of our network model for the severe example shown in Figure 1. In the case of emphysema, the situation is reversed. In mild emphysema (Figure 4, *middle right*) the lung is punctuated by islands of low density, whereas in severe disease (Figure 4, *bottom right*) these islands are juxtaposed to form a pathway that crosses the entire lung field, again resembling the network structure diagrammed in Figure 2. The same feature is apparent in the scanning electron micrograph of severely emphysematous tissue shown in Figure 5, in which one can see a contiguous series of large holes that contrast markedly with the uniform small-cell foamy appearance of normal tissue also shown in Figure 5. These globally spanning abnormalities, both in severe fibrosis and severe emphysema, again invoke the notion of discrete pathologic processes that have developed in number and size to the point at which they exceed their respective percolation thresholds. Thus, it is not just total lesional burden that progresses in these parenchymal diseases; organization of the lesions is also a key component of their pathophysiology.

One important implication of the percolation concept as applied to the lung concerns the heterogeneity of a disease process. As the concentration of the stiff springs increases in Figure 1, the spatial heterogeneity of the network structure, as seen in the examples shown in Figure 1, also increases until it reaches a maximum around the percolation threshold. Here, the network distortion can be substantial, with the retraction of groups of stiff springs creating large holes in some areas (*see* the fibrotic network animation in the online supplement) that might correspond to the classic peripheral honeycomb pattern seen on CT images of the severely fibrotic lung (30, 31). Beyond the percolation threshold, however, heterogeneity decreases until all the springs are stiff and the network has returned to complete homogeneity. This raises the possibility that texture variability in CT images might be used to identify patients with IPF close to the percolation threshold, and hence at risk of suffering an accelerated decline in lung function. The same concept also likely applies to emphysema. Indeed, CT images of lungs from emphysema patients exhibit enhanced regions of low attenuation that have an area distribution described by an inverse power law. The slope of this relationship in a log–log plot has been shown to be an indicator of early emphysema (32) as well as a good predictor of the outcome of lung volume reduction surgery (33).

It is appropriate to remember that our simple network model can describe reality only to a limited extent. For example, we have used the stiffness of the network as the primary functional readout of our simulations. However, the symptoms a patient

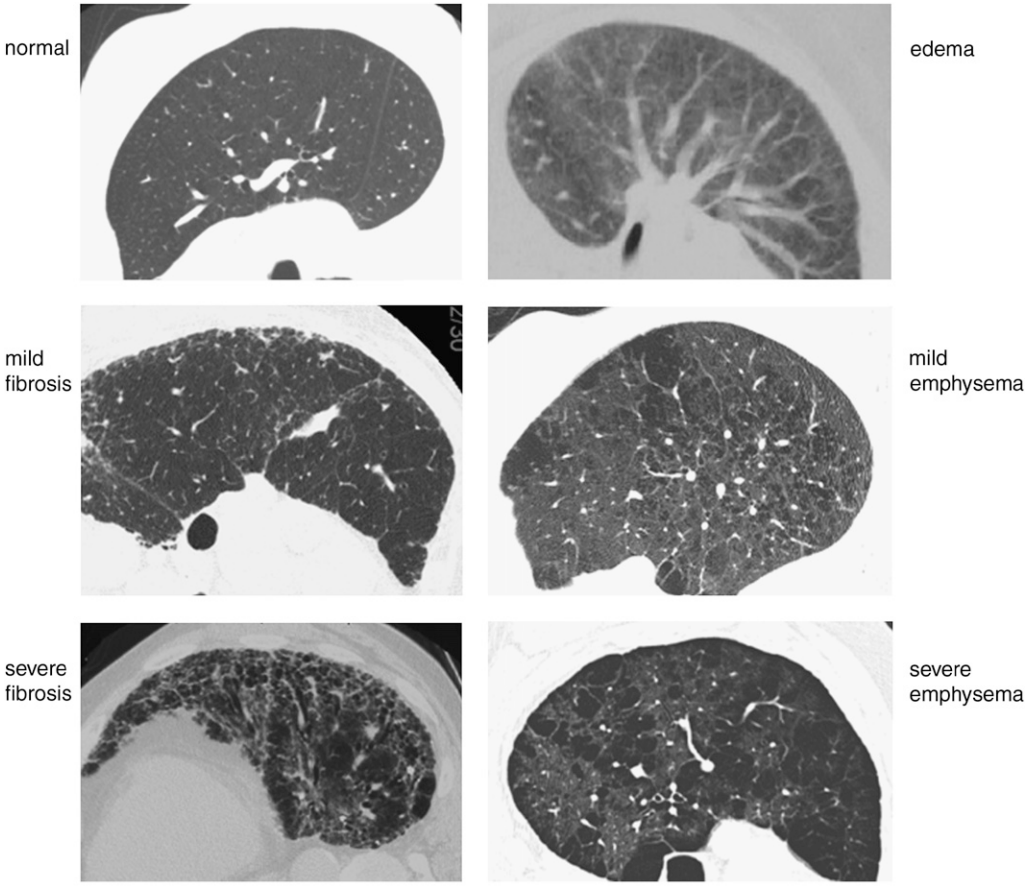

Figure 4. High-resolution computed tomography scan images illustrate diffuse or focal disease and percolation at a macroscopic level. Half-thorax images were selected from representative cases of the diseases of interest. Normal lung (*top left*) reveals gray lung parenchyma with numerous small structures of higher attenuation, linear septal planes, and blood vessels. Cardiac pulmonary edema (*top right*) appears as a diffuse hazy increase in tissue density involving the lung quite uniformly, and with prominent blood vessels. Mild usual interstitial pneumonitis (UIP) (*middle left*) shows focal areas of reticular opacities, particularly in a subpleural distribution, against a background of normal lung, whereas severe UIP (*bottom left*) shows extensive dense reticulation (honeycombing) spanning the cross-sectional plane. Mild emphysema (*middle right*) demonstrates enlarged airspaces (*black*) scattered throughout the normal (*gray*) tissue, whereas severe emphysema (*bottom right*) shows extensive widely linked large airspaces with little remaining normal tissue.

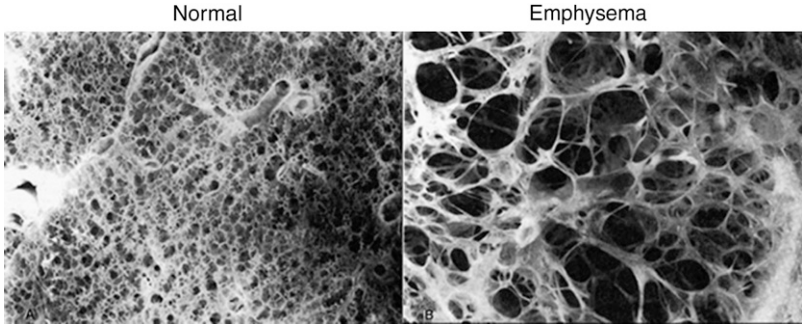

Figure 5. Scanning electron micrographs of normal lung tissue (*left*) and tissue from a lung with advanced emphysema (*right*). The emphysematous lung shows airspaces that vary in size from normal to greatly dilated. The abnormalities appear to be contiguous and extend across the entire field of view. Reprinted by permission from Reference 39.

experiences as either fibrosis or emphysema develops are complicated reflections of many factors in addition to lung compliance, including those determining peak flow rates, dynamic hyperinflation, and total lung capacity. The latter quantity is a function of the pressure–volume relationship of the lung. The equivalent for our spring network model is its relationship between force per unit perimeter length and area. We confirmed (data not shown) that this relationship is linear at all stages of either spring stiffening or cutting because the springs are linearly elastic. Accordingly, the predicted changes in B for fibrosis (Figure 1) and emphysema (Figure 2) are equivalent to proportional changes in lung compliance, and correspondingly to proportional changes in total lung capacity. Of course, the pressure–volume relationship of a real lung is highly curvilinear, due in large part to the progressive loading of previously flaccid collagen fibers with increasing lung volume (12). In principle, we could investigate the effects of such a mechanism in our network model (22), although this would pose significant computational challenges and greatly complicate the study. In any case, it seems clear just from consideration of the linear network behavior that percolation of developing lesions in lung tissue could induce sudden changes in total lung capacity.

One could also take issue with the fact that we altered the springs in the network in a completely random fashion in our simulation of fibrosis. Fibrotic lesions would exhibit spatial correlation if new lesions have a propensity to develop near existing ones rather than in the middle of completely normal tissue. We tested this possibility in the network model and found that although the qualitative picture does not change, the percolation threshold occurs at a lower concentration of stiff springs. We did invoke correlated development of pathology in our simulations of emphysema by allowing the preferential breaking of alveolar walls experiencing the greatest stress, as previous modeling studies have shown that this leads to lesional patterns similar to those seen in CT images in advanced emphysema (19).

Our network model also contains significant simplifications in terms of its mechanical behavior. We idealized this behavior in terms of a two-dimensional network of Hookean (strain-independent stiffness) springs. The hexagonal pattern of the network makes it structurally underdetermined, as is appropriate for a material whose shear modulus is substantially less than its bulk modulus (34). The stability problem was avoided by fixing the outer boundary of the network and applying a prestress to each spring. On the other hand, the parenchyma is both viscoelastic (35) and mechanically nonlinear (12, 22), yet we ignored these complications on the supposition that they do not fundamentally affect the validity of the percolation concept. They likely do affect, however, important details such as when the percolation threshold is reached and how sharply it alters mechanical behavior. We also modeled the lung parenchyma in only two dimensions, whereas the lung is a three-dimensional organ. On the other hand, the elastic properties of the lung arise largely from the stretching of essentially two-dimensional alveolar walls, so in a sense the lung can be viewed as a convoluted two-dimensional surface compacted into the thoracic space. Nevertheless, our model remains a highly simplistic representation of a tissue that exhibits structural complexity over a wide range of length scales. Accordingly, the mechanical behavior of the model can be taken to mimic that of the lung only in the broadest sense.

We also need to point out that the spring fraction scale shown in Figures 1 and 2 is not equivalent to the time scale of the progression of the disease process itself. For example, the early stages of chronic obstructive pulmonary disease are inflammatory in nature and tend to be protracted as the lung tries to repair the ongoing insults of smoking (11). This would be expected to temporally extend the early shoulder of the emphysema modulus curve shown in Figure 2, slowing the approach of the percolation threshold and its attendant clinical consequences. Despite all these simplifications, however, the simulated network structures are distinctly reminiscent of images of the fibrotic and emphysematous lungs shown in Figures 3–5, implying that percolation plays a role in the emergence of altered lung function in diseases of the parenchyma.

In conclusion, we have shown how the process of percolation, and in particular its emergent consequence known as the percolation threshold, can be invoked to account for the way in which progression of parenchymal lung disease might become disconnected from changes in lung mechanical function. Our results point to the importance of considering how the spatial organization of parenchymal pathology, in addition to its overall magnitude, impacts on our understanding of the link between structure and function in diseases such as IPF and chronic obstructive pulmonary disease. Indeed, there remains much from the field of complexity theory, as developed in a general sense by individuals such as Prigogine and Stengers (36) and Kauffman (37), that needs to be brought to bear on the study of lung pathology (38). Our results also underscore the notion, suggested in previous studies (3), that lack of ongoing decrement in lung function cannot be taken as lack of progression of the disease itself. The decision to treat may sometimes need to rest more on histologic or radiologic markers of disease status than on symptoms.

Conflict of Interest Statement: None of the authors has a financial relationship with a commercial entity that has an interest in the subject of this manuscript.

Acknowledgment: The authors thank Curtis Green, M.D., for supplying the high-resolution CT images.

References

1. Collard HR, King TE Jr, Bartelson BB, Vourlekis JS, Schwarz MI, Brown KK. Changes in clinical and physiologic variables predict survival in idiopathic pulmonary fibrosis. *Am J Respir Crit Care Med* 2003;168:538–542.

2. Piquette C, Rennard S, Snider G. Chronic bronchitis and emphysema. In: Murray J, Nadel J, Mason R, and Boushey H, editors. Textbook of respiratory medicine, 3rd ed. Philadelphia, PA: WB Saunders; 2000. pp. 1187–1245.
3. Martinez FJ, Safrin S, Weycker D, Starko KM, Bradford WZ, King TE Jr, Flaherty KR, Schwartz DA, Noble PW, Raghu G, *et al.* The clinical course of patients with idiopathic pulmonary fibrosis. *Ann Intern Med* 2005;142:963–967.
4. Srinakarin J, Thammaroj J, Boonsawat W. Comparison of high-resolution computed tomography with pulmonary function testing in symptomatic smokers. *J Med Assoc Thai* 2003;86:522–528.
5. Sashidhar K, Gulati M, Gupta D, Monga S, Suri S. Emphysema in heavy smokers with normal chest radiography: detection and quantification by HCRT. *Acta Radiol* 2002;43:60–65.
6. Verbeken EK, Cauberghs M, Lauweryns JM, Van de Woestijne KP. Structure and function in fibrosing alveolitis. *J Appl Physiol* 1994;76: 731–742.
7. Kelly SM, Bates JH, Michel RP. Altered mechanical properties of lung parenchyma in postobstructive pulmonary vasculopathy. *J Appl Physiol* 1994;77:2543–2551.
8. Wright JL, Churg A. Smoke-induced emphysema in guinea pigs is associated with morphometric evidence of collagen breakdown and repair. *Am J Physiol* 1995;268:L17–L20.
9. Michel RP, Goldberg P. Pulmonary edema. In: Hamid Q, Shannon J, and Martin JG, editors. Physiologic basis of respiratory disease. Hamilton, ON, Canada: BC Decker; 2005. pp. 203–236.
10. Gonzalez A, Ludwig M. Structure–function correlations in pulmonary fibrosis. In: Hamid Q, Shannon J, and Martin JG, editors. Physiologic basis of respiratory disease. Hamilton, ON, Canada: BC Decker; 2005. pp. 77–84.
11. Cosio MG, Saetta M, Ghezzo H, Baraldo S. Structure–function relationships in chronic obstructive pulmonary disease. In: Hamid Q, Shannon J, Martin JG, editors. Physiologic basis of respiratory disease. Hamilton, ON, Canada: BC Decker; 2005. pp. 85–104.
12. Maksym GN, Bates JH. A distributed nonlinear model of lung tissue elasticity. *J Appl Physiol* 1997;82:32–41.
13. Mead J. Mechanical properties of lungs. *Physiol Rev* 1961;41:281–330.
14. Janssen HK, Muller M, Stenull O. Generalized epidemic process and tricritical dynamic percolation. *Phys Rev E Stat Nonlin Soft Matter Phys* 2004;70:026114.
15. Coniglio A, de Candia A, Di Talia S, Gamba A. Percolation and Burgers' dynamics in a model of capillary formation. *Phys Rev E Stat Nonlin Soft Matter Phys* 2004;69:051910.
16. Tang W, Thorpe MF. Percolation of elastic networks under tension. *Phys Rev B Condens Matter* 1988;37:5539–5551.
17. Bates J, Davis G, Majumdar A, Suki B. Percolation of parenchymal lung disease and its effects on changes in mechanical function [abstract]. Presented at the annual fall meeting of the Biomedical Engineering Society, September 28–October 1, 2005, Baltimore, MD. Proceedings talk no. 936.
18. Cavalcante FS, Ito S, Brewer K, Sakai H, Alencar AM, Almeida MP, Andrade JS Jr, Majumdar A, Ingenito EP, Suki B. Mechanical interactions between collagen and proteoglycans: implications for the stability of lung tissue. *J Appl Physiol* 2005;98:672–679.
19. Suki B, Lutchen KR, Ingenito EP. On the progressive nature of emphysema: roles of proteases, inflammation, and mechanical forces. *Am J Respir Crit Care Med* 2003;168:516–521.
20. Zekri N, Porterie B, Clerc JP, Loraud JC. Propagation in a two-dimensional weighted local small-world network. *Phys Rev E Stat Nonlin Soft Matter Phys* 2005;71:046121.
21. Bachofen H, Hildebrandt J, Bachofen M. Pressure–volume curves of air- and liquid-filled excised lungs: surface tension *in situ*. *J Appl Physiol* 1970;29:422–431.
22. Maksym GN, Fredberg JJ, Bates JH. Force heterogeneity in a two-dimensional network model of lung tissue elasticity. *J Appl Physiol* 1998;85:1223–1229.
23. Arbabi S, Sahimi M. Elastic properties of three-dimensional percolation networks with stretching and bond-bending forces. *Phys Rev B Condens Matter* 1988;38:7173–7176.
24. Wilson TA, Bachofen H. A model for mechanical structure of the alveolar duct. *J Appl Physiol* 1982;52:1064–1070.
25. Anthonisen NR, Connett JE, Kiley JP, Altose MD, Bailey WC, Buist AS, Conway WA Jr, Enright PL, Kanner RE, O'Hara P, *et al.* Effects of smoking intervention and the use of an inhaled anticholinergic bronchodilator on the rate of decline of FEV_1: the Lung Health Study. *JAMA* 1994;272:1497–1505.
26. Foronjy RF, Mercer BA, Maxfield MW, Powell CA, D'Armiento J, Okada Y. Structural emphysema does not correlate with lung compliance: lessons from the mouse smoking model. *Exp Lung Res* 2005;31:547–562.
27. Corbin RP, Loveland M, Martin RR, Macklem PT. A four-year follow-up study of lung mechanics in smokers. *Am Rev Respir Dis* 1979;120:293–304.
28. Fletcher C, Peto R. The natural history of chronic airflow obstruction. *BMJ* 1977;1:1645–1648.
29. Shapiro SD, Ingenito EP. The pathogenesis of chronic obstructive pulmonary disease: advances in the past 100 years. *Am J Respir Cell Mol Biol* 2005;32:367–372.
30. Coxson HO, Hogg JC, Mayo JR, Behzad H, Whittall KP, Schwartz DA, Hartley PG, Galvin JR, Wilson JS, Hunninghake GW. Quantification of idiopathic pulmonary fibrosis using computed tomography and histology. *Am J Respir Crit Care Med* 1997;155:1649–1656.
31. Akira M, Sakatani M, Ueda E. Idiopathic pulmonary fibrosis: progression of honeycombing at thin-section CT. *Radiology* 1993;189:687–691.
32. Mishima M, Hirai T, Itoh H, Nakano Y, Sakai H, Muro S, Nishimura K, Oku Y, Chin K, Ohi M, *et al.* Complexity of terminal airspace geometry assessed by lung computed tomography in normal subjects and patients with chronic obstructive pulmonary disease. *Proc Natl Acad Sci USA* 1999;96:8829–8834.
33. Coxson HO, Whittall KP, Nakano Y, Rogers RM, Sciurba FC, Keenan RJ, Hogg JC. Selection of patients for lung volume reduction surgery using a power law analysis of the computed tomographic scan. *Thorax* 2003;58:510–514.
34. Stamenovic D. Micromechanical foundations of pulmonary elasticity. *Physiol Rev* 1990;70:1117–1134.
35. Hildebrandt J. Pressure-volume data of cat lung interpreted by a plastoelastic, linear viscoelastic model. *J Appl Physiol* 1970;28:365–372.
36. Prigogine I, Stengers I. Order out of chaos. New York: Bantam Books; 1984.
37. Kauffman S. At home in the universe. Oxford, UK: Oxford University Press; 1995.
38. Macklem PT. Complexity and respiration: a matter of life and death. In: Hamid Q, Shannon J, Martin J, editors. Physiologic basis of respiratory disease. Hamilton, ON, Canada: BC Decker; 2005. pp. 605–609.
39. West J. Pulmonary pathophysiology: the essentials, 6th ed. Baltimore, MD: Lippincott, Williams & Wilkins; 2003.